Effect of Cd^{2+} Substituted Nickel Ferrite oxide ($Ni_{1-x}Cd_xFe_2O_4$) on Magnetic, Dielectric and Structural Properties

K.R. Kharat[1], S.L. Jadhav[2], A.L. Jadhav[3], A.V. Kadam[3], J.L. Bhosale[4], T.S. Magdum[5*]

[1] Department of Physics, Prof. Dr. N.D. Patil Mahavidyalaya, Malkapur-415101, India.

[2] Department of Physics, D.P.Bhosale College, Koregaon, Satara, 415501, India.

[3] Department of Physics,The institute of science, Mumbai (Dr. Homi Bhabha state University), 15, Madam Cama Road, Mumbai-400 032. India.

[4] Department of Physics, Shikshanmaharshi Dr. Bapuji Salunkhe College, Miraj-416410, India.

[5] Department of Physics, Yashwantrao Chavan Mahavidyalaya, Halkarni-416552, India.

*Corresponding author

doi: https://doi.org/10.21467/proceedings.118.57

ABSTRACT

The effect of cadmium (Cd^{2+}) substituted at the $NiFe_2O_4$ nano materials were this nano material synthesized by auto-combustion technique. The structural analysis confirms that the samples are polycrystalline nature with spinel cubic crystal symmetry. The effect of Cd^{2+} contains on lattice constants which obeys Vegard's law. The morphological analysis shows that the highly porous structure with spongy like surface morphology. The observed absorption infrared spectra confirm that the exhibits the nano ferrite materials. The magnetic properties measurements reveal that the saturation of magnetization decreases with an increase in constituent Cd^{2+} in nickel ferrous oxide. The Cd^{2+} ions present in A-site and Fe^{3+} are distributed in both tetrahedral and octahedral sites of spinel lattice. The DC measurement shows that the semiconducting behaviour of the prepared $Ni_{1-x}Cd_xFe_2O_4$. The increase in Cd^{2+} constituent in the nickel ferrite with decrease curie temperature. The dielectric measurement of all samples shows the usual dielectric dispersion with frequency. The impedance spectroscopy analysis suggests grain interior contribution in the conduction process.

Keywords: Auto-Combustion; Ni-Cd ferrite oxide; XRD; FT-IR; Magnetic properties, Dielectric.

1 Introduction

In recent years, the developments of modern high-speed communication system and various electronic equipment have been accountable for increases pollution of the microwave radiations. Consequently, several researches have been done on creating microwave radiations absorbing materials. In a recent microwave radiation absorbing materials must be spinel ferrite nano composite materials because these ferrite nano composite materials show several properties of magnetism, dielectric loss and dc conductivity etc. [1]. In general, microwave radiation absorbing nano composite materials describes by two-way (a) magnetic and (b) dielectric materials. The ferrites nano composite materials are excellent for microwave radiations absorption may be due to their unique properties of the magnetism behaviors. In the ferrite materials exhibits the magnetizations due to unpaired electrons of transition metal. The exchanges of spins between tetrahedral (A), octahedral (B) sites are known as super exchange magnetic interaction (SEMI). The Mossbauer spectrum technology shows two independent different distributions of effective fields with the relative area of ferric contributions site(A) and Site(B), it is shows existing of reversed magnetic moments in octahedral sites same result observed by Grenche et.al [2].

The nickel ferrite is the low cost soft magnetic material and has significant magnetic and electrical properties. The so many properties of ferrites such as magnetization behaviours, low dielectric losses, Curie temperature, and DC resistivity. These properties are based on the ionic composition of material, heat

Proceedings DOI: 10.21467/proceedings.118; Series: AIJR Proceedings; ISSN: 2582-3922; ISBN: 978-81-947843-6-4

treatment, and type of substituted ions in the synthesized composite materials. Cd-Ni ferrite oxide has a spinal structure, in which tetrahedral A-sites are of a building by Cd^{2+}, Ni^{2+} ions, and octahedral B-sites are of a building by Fe^{3+} ions [3]. The substitution of other metal ions has been commonly used to modify the physicochemical, electrical, and magnetic properties in the ferrite. The chemical composition structural formula for spinel ferrites is $Ni_{1-x}Cd_xFe_2O_4$ where x is the inversion parameter. The inversion parameter for the normal spinel is zero and inverse spinel is one. Several reports show improvement in these properties such as electric, magnetic and dielectric losses of substituted nickel ferrite [4]. Their properties of the ferrite nano material as well depend on the cation's distribution and additionally paucity in the chemical's composition [5]. Among all the ferrites, cadmium substituted nickel ferrite is considered to be the most adaptable and found broad extend purpose in the electronics and microwave absorbing devices due to high electrical resistivity, low eddy current, and shows excellent dielectric loss [6-9]. Nickel-cadmium ferrite oxide is widely used in many technological and applications such as magnetic disks, receiver antenna, induction coils, microwave absorbing devices, core transformers. The ferrite nano material can be synthesized by various chemical methods such as double sintering ceramic method [10], co-precipitation [11], hydrothermal [12] Sol-gel [13], organometallic precursor [14], citrate precursor [15], gel auto-combustion [16], etc.

The simplest sol-gel method has been used to preparations of the high-quality spinel ferrite nano materials with better properties such as lower preparation temperatures, shorter times, homogeneity, purity of materials and reduced its cost [13]. This method involves the oxidation/reduction process of aerogel, which is obtained from an aqueous solution consisting of oxidizers such as desired metal salts and reductant such as organic complexant. During aerogel combustion, the rapid growth of a huge volume of gases leads to the construction of nano particles. Also, the line intensity of the in-field gives strong evidence for a ferromagnetic structure up to x=0.30 composition. The cations distribution and physicochemical properties of Ni-Cd ferrite nanoparticles by employing a citrate gel process same result observed by Lohar *et al.* [17]. They confirmed that the Ni-Cd samples are suitable material for the recording heads and antenna rods application due to its soft magnetic behaviour. The magnetic properties ferrites will be improved by substituting the other metal ions into the host lattice. Cd^{2+} is a nonmagnetic ion and a very capable candidate in them. In my research article, the composite of Nickel Cadmium ferrite is a co-mixed spinel structure here in the effect of cadmium can modify the electric, dielectric and magnetic behaviors.

Our best knowledge, very little work found on cadmium doped at the nickel ferrite oxide for the structural magnetic and dielectric properties. However, some works on dielectric properties of Ni–Zn, Ni-Cd, and Mn–Zn ferrites have been reported [18-20]. We have in this research work carried out two different way, initially we employed auto gel combustion route for the synthesis of the cadmium doped nickel ferrite oxide ($Ni_{1-x}Cd_xFe_2O_4$) nano material. Another, we have study of the effect of cadmium substituted in the nickel ferrite oxide on the structural, magnetic, dielectric constant with dielectric loss.

2 Experimental procedure

Samples of $Ni_{1-x}Cd_xFe_2O_4$ (X=0.0 to 0.5) were prepared by the sol-gel auto combustion route. A mixture of chemical composition solution prepared in double-distilled water $Fe(NO_3)_3.9H_2O$, with $Ni(NO_3)_2.6H_2O$ and $Cd(NO_3)_2.6H_2O$ in an appropriate proportion was taken. The prepared mixture of chemical composition solution was stirred on a magnetic stirrer for 3 hr and to get a uniform combination of chemical compositions. Further, the glycine solution (fuel) was slowly added into the obtained chemical combinations due to the formation of a redox mixture. The solution was then dehydrated gradually onto a hot plate with continuous stirring then the sticky gel was formed. Further, the prepared sticky gel at a particular temperature auto-explosion (fire) of the black ash and finally gets fluffy gel took place in the

beaker. The obtained powder was grinding for 40 min and sintered at the 1000°C for 6 h in a programmable auto furnace. Then the powder is hard-pressed into the pellets by using a 4% PVA binder and by applying pressure of near about 6 ton for 6 min. These pellets were finally sintered at 1100°C for 10 hr to reduce porosity, the present PVA binder vaporized, and increase density. These prepared samples were further used for studying structural, electrical, magnetic, and dielectric properties.

2.1 Characterization Techniques

The structural properties were studied by Bruker D2-Phaser X-ray diffractometer (XRD) with Cu-K〈 radiation (λ=1.5406 Å). The surface morphological images carried out by using a Field emission scanning electron microscope (FE-SEM) (Mira-3, Tescan, Brno-Czech Republic). The DC electrical resistivity was estimated by utilizing the two-probe meter with highly sensitive Keithley electrometer model-6514. The Fourier transform infrared spectra (FTIR) were recorded in the range 360–1000 cm^{-1} at room temperature using the Alpha-100508 spectrometer. The magnetic properties of all samples were explored using a vibrating sample magnetometer (VSM) Lakeshore-7000 model. The dielectric measurements were carried out using a high precision LCR meter bridge model-HP-6284A in the frequency range 20Hz to 1MHz.

3 Results and discussion

3.1 X-ray diffraction study

The structural analysis of these prepared sample ferrites ($Ni_{1-x}Cd_xFe_2O_4$) was carried out by using X-ray diffraction technique on Rigaku, diffractometer (Cu-$K\alpha$ radiation, λ =1.540562Å, $2\theta = 20^0$ - 80°). Fig.1. shows the lattice peak are (111), (220), (222), (311), (400), (422), (511), and (440). It indicates that the formation of spinel cubic structure similarly results observed by M. De et.al [21]. It is also seen that the intensity of the peak lattice planes decreases with an increase in Cd^{2+}concentration due to no other reflection's peaks are observed in all samples. In fig.1 clearly shows the (311) peak position is slightly shifted towards the lower angle side due to the linear increase in the lattice constant upon increasing Cd^{2+} content which is the observed result match with good agreement with Vegard's law [22]. The crystallite size (*D*) was estimated from the XRD peak broadening of the lattice peak (311) by using Debye Scherrer's relation [23].

$$D = \frac{0.9*\lambda}{\beta cos\emptyset}$$

Where, k = 0.9 is the Scherrer's constant, λ =1.540562Å is the wavelength of X-rays and β is the full-width half maxima (FWHM) of the lattice peak at an angle. The average crystallite size (*D*) has been calculated using Scherer's formula given as 42.8 nm,38.6 nm,35.5nm,33.2 nm,31.2 nm, and 29.8 nm for the Cd^{2+}(0.0% to 0.5%) doped nickel ferrite.

Proceedings DOI: 10.21467/proceedings.118
ISBN: 978-81-947843-6-4

Series: AIJR Proceedings
ISSN: 2582-3922

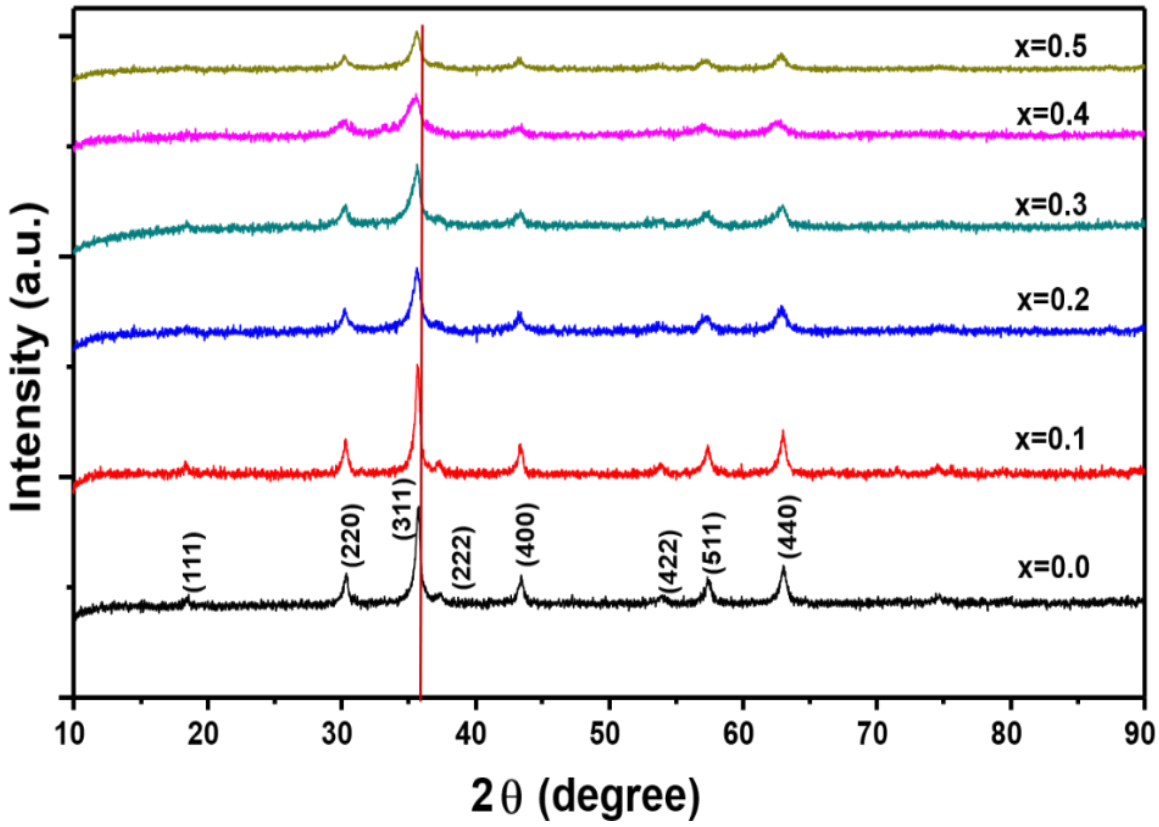

Figure 1 X-ray diffraction patterns of $Ni_{1-x}Cd_xFe_2O_4$ (x=0.0 to 0.5) ferrite system

The crystallite size increases with increasing Cd^{2+} content in nickel ferrite due to Cd^{2+} ions occupy A-sites. The lattice constant of all samples was determined by using the formula [24].

$$a = d\sqrt{h^2 + k^2 + l^2} \quad (1)$$

Where, '*a*' is the lattice constant, (hkl) represents the Miller indices and d represents the interplanar distance. The values of lattice constant (*a*) increased with increasing Cd^{2+} content in nickel ferrite. The observed values of lattice constant are in good agreement with those reported in the literature [25]. The tetrahedral and octahedral bond lengths R_A, R_B, and ionic radii r_A, r_B of the samples are calculated by using XRD data and depicted in similarly relation used Hemant Kumar Dubey et.al [13]. Table 1. The bond lengths R_A, R_B, and ionic radii r_A, r_B of A-site and B-site was increased linearly due to the increase in lattice constant concerning Cd^{2+} content.

3.2 Field Emission Scanning Electron Microscopy

Fig.2.the micrographs of prepared $Ni_{1-x}Cd_xFe_2O_4$ ferrite samples by auto combustion route analyzed by using FE-SEM microscopy. The samples contained cotton cluster-like structures. The existence of cotton clusters in the synthesized nanoparticles may be recognized as the magnetic dipole interaction with the nearby nanoparticles. It is evident from FE-SEM investigation that the grain of nickel cadmium ferrite is in nanoscale with striking pores. The voids and mesopores present in the examples could be recognized for the release of gases during the explosion process.

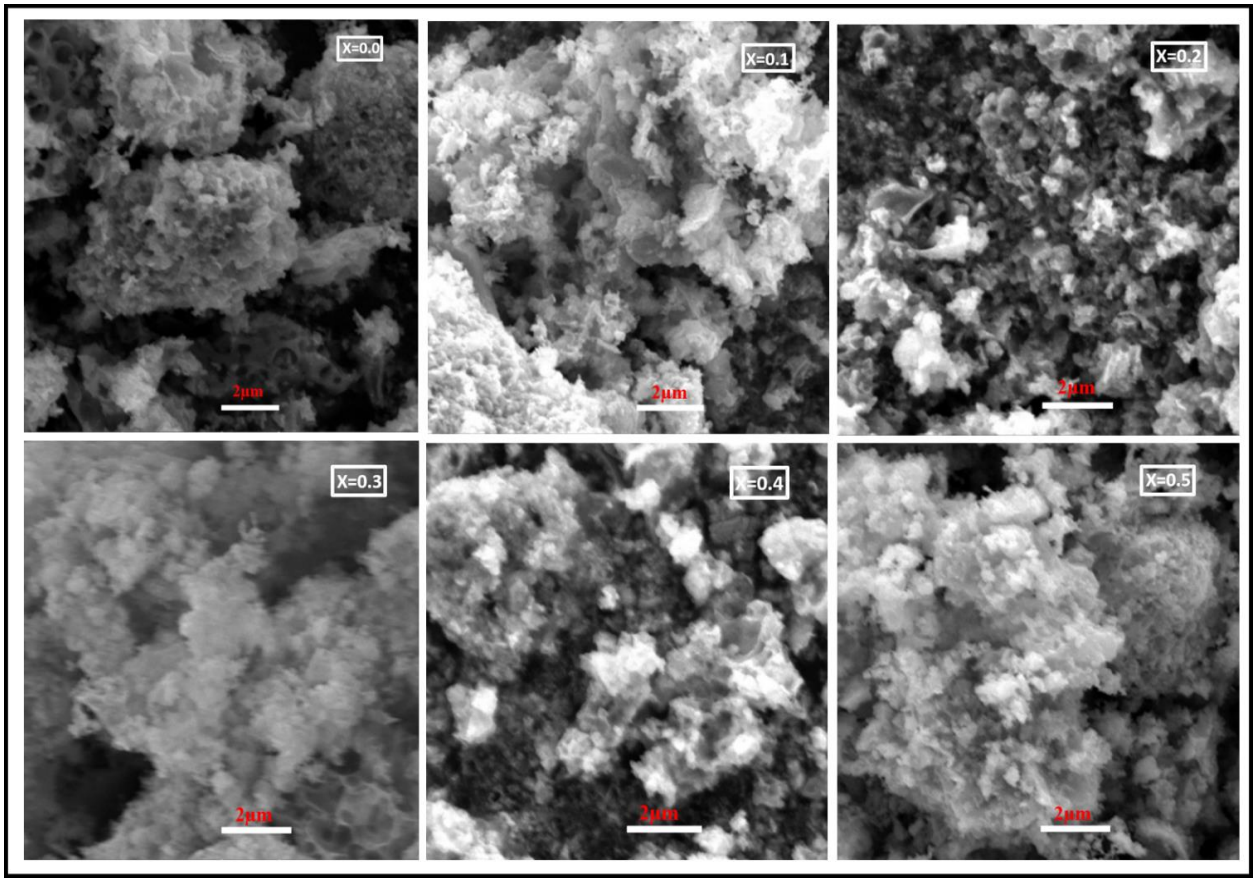

Figure 2 FE-SEM images of $Ni_{1-x}Cd_xFe_2O_4$ (x=0.0 to 0.5) ferrite system

From the micrographs, one can particularly see that the morphological changes occur with varying Cd content (x) in $Ni_{1-x}Cd_xFe_2O_4$. In the few samples with x = 0.0 and 0.5, one can see that the grains are very much isolated. By addition of Cd^{2+} the grain size increases along with a packet of the cotton spheres. The average particle size of the ferrite system was found to be 0.5–1.0 μm. The observed disparity in grain size is accredited to the grain-growth mechanism involving diffusion coefficients and the concentration of dissimilar ions. Besides, we utilized the energy-dispersive X-ray (EDAX) spectroscopy, which is used to investigate the chemical composition for the constituent elements of the synthesized nanomaterials. The EDAX result (Fig.3) confirmed the presence of elements Ni, Cd, Fe, and O without any impurity. The atomic weight % of major elements presented inside the EDAX spectra corroborates the formation of Ni-Cd ferrite.

Proceedings DOI: 10.21467/proceedings.118
ISBN: 978-81-947843-6-4

Series: AIJR Proceedings
ISSN: 2582-3922

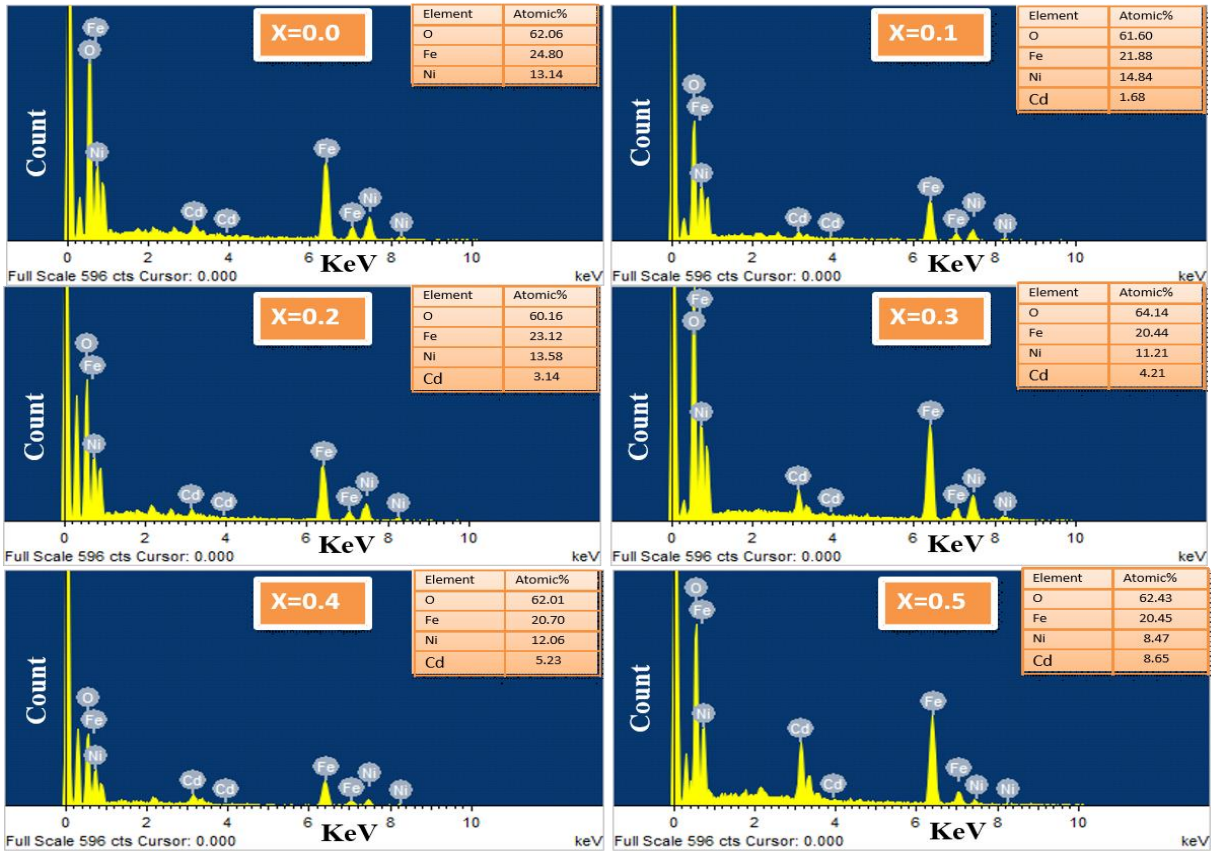

Figure 3 EDAX spectra of $Ni_{1-x}Cd_xFe_2O_4$ (x=0.0 to 0.5) ferrite system

3.3 FTIR analysis

To validate the formation of spinel structure and to look at the chemical properties of the material, the infrared (IR) spectroscopy of Cd^{2+} substituted nickel ferrite was carried out. The analysis of IR spectra can give information about the structural modification and to get information about the position of cations in the spinel lattice. The IR spectra of $Ni_{1-x}Cd_xFe_2O_4$ (x=0.0 to 0.5) ferrite system is shown in Fig. 4.

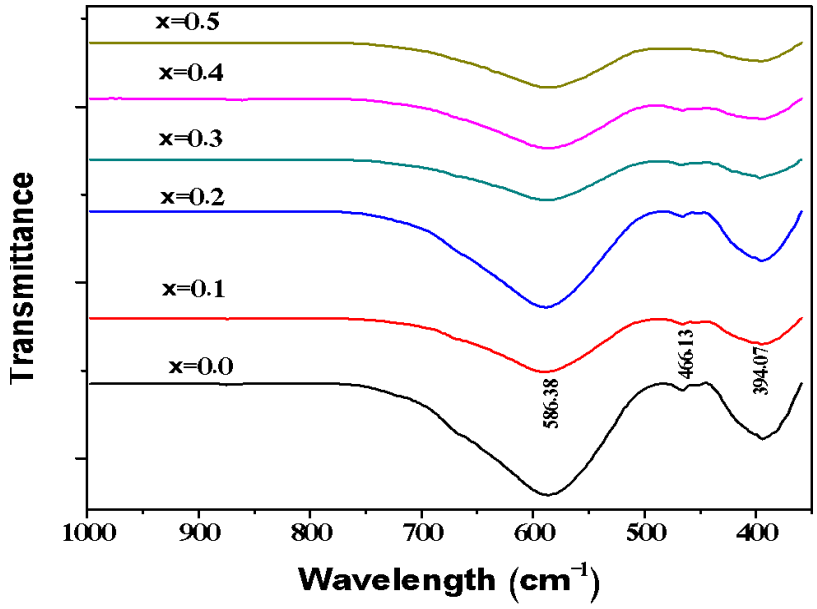

Figure 4 FTIR spectra of $Ni_{1-x}Cd_xFe_2O_4$ (x=0.0 to 0.5) ferrite system

The spectra show the two strong characteristic absorption bands in the range of about 600 to 400cm^{-1}. The highest concentrated band is observed at about 586 cm^{-1} (υ_1) which correspond to intrinsic stretching vibrations of the metal ions and oxygen at the tetrahedral A-site as well as lowest band is observed at about 394 cm^{-1} (υ_2) which correspond to metal-oxygen stretching vibrations of octahedral B-site [26]. When Cd^{2+} content in the nickel ferrite was increases as the result the highest band is transferred towards a higher frequency side and but the position of the lowest band does not much change. It takes place due to the larger ionic radii of Cd^{2+} than Ni^{2+} ions at octahedral A-site, the Cd^{2+} ion occupies only the tetrahedral A-sites and it remains constant at the interstitial A-sites, this leads to an increase in the highest band towards higher frequency side. Similar IR spectra of the metal ion substituted nickel ferrite were reported in Pachpinde et.al [27]. The slight variation in the position and intensities of the highest absorption bands is due to the difference in the Fe^{3+}-O and Cd^{2+}-O distances from A-sites. The divergence in the band position is predictable because of the difference in the Fe^{3+}-O^{2-} distances for the octahedral A-sites. The distinction in lattice constant and cation distribution is responsible for the band shift of the centre frequency. The increase in the unit cell dimensions due to the replacement of Ni^{2+} ions by Cd^{2+} ions affect the Ni^{2+}-O^{2-} stretching vibration which causes the change in higher band position. The varying in the frequency of the υ_1 stretching band shows that the first choice of Cd^{2+} ions and occupies the tetrahedral A-sites.

3.4 DC electrical resistivity

To the measurement of the DC electrical resistivity of the prepared spinel ferrite materials. The nickel ferrite materials exhibit high resistive behaviours [28], but some ferrite materials show low DC resistivity, enhancing the resistivity of the materials could be additions of trivalent or divalent atoms at sites of ferrite materials. These resistivity properties of $Ni_{1-x}Cd_xFe_2O_4$ dependent on the temperature shown in Fig.5(a)it is clearly show that the Arrhenius plot. The resistivity is depending on temperature which demonstrated the semiconducting character. The decreases resistivity of the $Ni_{1-x}Cd_xFe_2O_4$ with increase in temperature may be due to an increase's mobility of charge carriers [21]. The measured DC resistivity plots (Fig.5(a)) shows the two temperature regions and their slopes will be different. At lower temperatures clearly show that ferromagnetic states and at the higher temperature shows disordered paramagnetic nature. The activation energy (ΔE) was calculated in two different temperature i.e., ferromagnetic and paramagnetic region are tabulated in Table I. The tabulated values indicates that the activation energies of the paramagnetic region are higher than the ferromagnetic region due to disordering states [29] and are in good conformity with the theory of Irkin and Turor et.al [30].

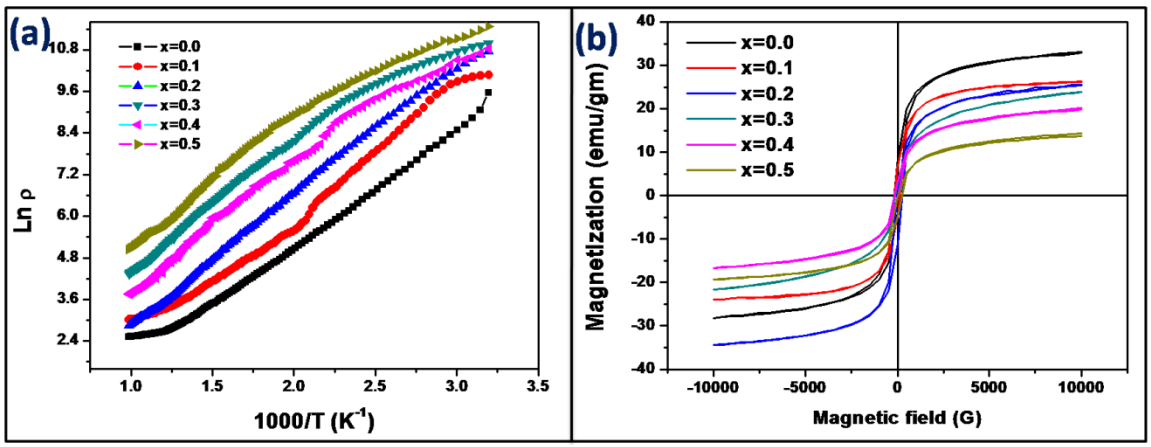

Figure 5(a).DC electrical resistivity with temperature of $Ni_{1-x}Cd_xFe_2O_4$ (x=0.0 to 0.5) ferrite system,**(b)**M-H curves of $Ni_{1-x}Cd_xFe_2O_4$ (x=0.0 to 0.5) ferrite system measured at room temperature

Proceedings DOI: 10.21467/proceedings.118
ISBN: 978-81-947843-6-4

Series: AIJR Proceedings
ISSN: 2582-3922

Also, the activation energy increase is confirmed that the barriers energy increase for hopping electrons, these results show increases the DC resistivity of the spinel ferrite materials. The Curie temperature (*Tc*) of the ferrite system varies from 550° to 615°C as shown in Table 1. In ferrite materials, all of the values of *Tc* depend on the subsistence of a cations and bond strength of these sites. The effect of cadmium doped nickel ferrite spinel material, the Ni^{2+} ions are replaced by Cd^{2+} ions hence increase in the strength of the site A and site B interaction without changes B-site Fe^{3+} ions. The Curie temperature decrease with an increase in Cd^{2+} content in nickel ferrites. The conduction below Curie temperature is due to the hopping of electrons between Fe^{2+} and Fe^{3+} ions, whereas, above Curie temperature, the conduction is due to the polarons hopping [31]. The decreases in Curie temperature *(Tc)* for increase in Cd^{2+}substitution for another spinel ferrite was observed by Lohar *et al.* [17]

Table I: Lattice constant, crystallite size, ionic radii, bond length, activation energy and Curie temperature of $Ni_{1-x}Cd_xFe_2O_4$ (x=0.0 to 0.5) ferrite system

Cd^{2+} Content (x)	Lattice constant (A^0)	Crystallite size D (nm)	r_A (A^0)	r_B (A^0)	R_A (A^0)	R_B (A^0)	Activation energy ΔE (eV)		Curie temperature T_c ^{0}(C)
							Ferromagnetic region	Paramagnetic region	
0.0	8.3214	45	1.8881	2.031	0.5381	0.6804	0.24	0.28	615
0.1	8.3421	49	1.8928	2.033	0.5428	0.6854	0.28	0.35	597
0.2	8.3549	58	1.8957	2.039	0.5457	0.6885	0.26	0.37	589
0.3	8.3616	63	1.8972	2.041	0.5472	0.6902	0.33	0.35	581
0.4	8.3692	66	1.8989	2.043	0.5489	0.692	0.22	0.30	575
0.5	8.3739	72	1.9011	2.044	0.550	0.6932	0.38	0.39	550

3.5 Magnetic properties

Fig.5 (b). Shows M-H hysteresis curves of $Ni_{1-x}Cd_xFe_2O_4$ (x=0.0 to 0.5) ferrites materials at room temperature. The experimental magnetic parameters calibrated from hysteresis curves values are presented in Table II. The observed magnetization saturation and coercivity was observed with increases in Cd^{2+}concentration. This can be attributing to the superexchange interactions between divalent metal ions and Fe^{3+} ions in the octahedral site in the spinel lattice. The net magnetization in ferromagnetic substance was dependent not only on types but also on the located ions at the tetrahedral (A) and octahedral (B) sites. The loss of magnetization from x = 0.0 to x =0.5 with Cd^{2+} substitution due to the alternate of Ni^{2+} ions by Cd^{2+} ions with which in turn go down the resultant net magnetic moment. Additionally, the decrementation in the magnetization is might be due to the quenching of the total orbital momentum leaving the spins to the only efficacious parameter. So, one can expect that the more immensely colossal Cd^{2+} ions will prefer to occupy tetrahedral A-sites. When the Cd^{2+} substitution increased, the saturation magnetization reduced as compared with the pure nickel ferrite. It is due to the fact that nonmagnetic Cd^{2+} ions (0 μB) replace magnetic Ni^{2+} ions (2 μB) [32]. Cd^{2+} ions are highly non-magnetic; thus, the ferromagnetic region decreases at the expense of the paramagnetic region by superseding Ni^{2+} ions. The total magnetic moments in the ferrite spinel completely based on the number of magnetic ions fill in the tetrahedral and octahedral sites [33]. Also, the increasing crystallite size with an increase in Cd^{2+} ions lead to the increase of random spins which causes the reduction of magnetization. Since Cd^{2+} is a non-magnetic ion, it doesn't participate in the exchange interactions with its most proximate atom. Therefore, the

magnetic super-exchange interaction between the Cd^{2+} and Ni^{2+}cations decrease with the incrementation of concentration [34]. The lower value of the coercive field is observed for the composition x=0.2 composition. This can be attributed to the vicissitude in magneto-crystalline anisotropy due to the supersession of Ni^{2+} ions by Cd^{2+} ions from the A-site. After that, the coercive field (Hc) increases due to the increasing crystallite size with an increase in Cd^{2+} content. For bulk particles coercivity and crystallite size have reciprocal cognation [35]. The small coercive field predicts that it can be used in highly capable data storage devices because minimum coercivity allows writing and overwriting of data. In the present study, the variation of coercivity (Hc) and crystallite size (D) correlated with each other, and the coercivity which was found to be in the range of 73-256 G. Withal, the maximum value of the coercivity was visually perceived for the composition with x=0.0 which has crystallite size 45 nm while the minimum value of the coercivity was found to be for the composition at x=0.2 having crystallite size 58 nm. The coercivity of ferromagnetic ferrite depend on metal ions entering into the interstitial sites of spinel lattice, which may distort the lattice and generate an internal stress and the nonmagnetic ions have a vigorous spin-orbit coupling [36]. Therefore, the samples having coercivity Hc > 600 one was suitable for the application of magnetic recording media, and the samples of coercivity in the range 600-900 are suitable for switching circuit, sensor, and high microwave frequency applications [37]. The anisotropy constant (K) will depend on the Cd^{2+} ion concentration, which can be resolute by utilizing the well-known cognation [38] and values are presented in Table 2. The magnetic anisotropy of the material is directly proportional to the coercivity and variation is occurred with increasing Cd^{2+} content. The shape and region of the curve are directly associated with density, chemical composition, porosity, and grain size that in turn are influenced by annealing condition.

Table II: Cation distribution and magnetic parameter of $Ni_{1-x}Cd_xFe_2O_4$ (x=0.0 to 0.5) ferrite system.

Cd^{2+} content (x)	Cation Distribution	Ms (emu/gm)	Mr (emu/gm)	Hc (G)	Mr/Ms	Anisotropy constant K×10^3 (erg/g)
0.0	$(Fe_1^{+2})[Ni_1^{2+}Fe_1^{3+}])O_4^{-2}$	33.12	8.51	253	0.256	8.7
0.1	$(Cd_{0.1}^{2+}Fe_{0.9}^{+2})[Ni_{0.9}^{2+}Fe_{1.1}^{3+}])O_4^{-2}$	26.30	6.26	216	0.238	5.9
0.2	$(Cd_{0.2}^{2+}Fe_{0.9}^{+2})[Ni_{0.8}^{2+}Fe_{1.1}^{3+}])O_4^{-2}$	25.69	1.43	73	0.040	1.9
0.3	$(Cd_{0.3}^{2+}Fe_{0.9}^{+2})[Ni_{0.7}^{2+}Fe_{1.1}^{3+}])O_4^{-2}$	23.88	2.28	114	0.095	2.8
0.4	$(Cd_{0.4}^{2+}Fe_{0.9}^{+2})[Ni_{0.6}^{2+}Fe_{1.1}^{3+}])O_4^{-2}$	20.09	3.10	165	0.154	3.4
0.5	$(Cd_{0.5}^{2+}Fe_{0.9}^{+2})[Ni_{0.5}^{2+}Fe_{1.1}^{3+}])O_4^{-2}$	14.26	2.77	101	0.194	1.5

3.6 Dielectric properties

The dielectric properties such as real and imaginary part of dielectric constant (ε') and dielectric loss tangent (tan™) of all samples are studied at frequencies 20 Hz to 1 MHz. The real part of the dielectric constant (ε') was estimated by using the following equation [39].

$$\varepsilon' = \frac{C_p t}{\varepsilon_0 A} \qquad (2)$$

Proceedings DOI: 10.21467/proceedings.118
ISBN: 978-81-947843-6-4

Series: AIJR Proceedings
ISSN: 2582-3922

Where Cp is capacitance, t is thickness, A is be the area of the cross-section of the synthesized pellet and ε_0 is the permittivity of free space. Fig.6(a) shows the discrepancy of real part of dielectric constant (ε') with frequency in Hz of $Ni_{1-x}Cd_xFe_2O_4$ (x=0.0 to 0.5) system. The real part of the dielectric constant linearly decreases at lower frequencies and it remains constant at a higher frequencies region which clearly indicates that the common type of dielectric dispersion. This dielectric dispersion is also accredited to Maxwell–Wagner type [40, 41] polarizations included between the sites of the faces; this exhibits good agreement with Koop's theory [42]. The decrementation in ε' at low frequencies due to at some frequencies electric charge can't follow the vicissitudes of applied electric field and electron hopping between Fe3+ and Fe2+ ions in the ferrite materials. Due to the occurrence of Fe^{3+} and Fe^{2+} ions ferrite is termed as dipolar behaviour. The dipoles generate rotational dislodgment results in the orientation of polarization. The rotation of $Fe^{2+} \leftrightarrow Fe^{3+}$ dipoles can be fantastically as the exchange of ions so that the alignment of dipoles generates a replication to the applied alternating electric field [43]. In Ni-Cd ferrite, the Ni^{2+} ions present in tetrahedral A-site are responsible for decrementing in concentration of Fe^{3+} ions in octahedral B-site which minimizes the kineticism of Fe^{2+} to Fe^{3+}. Shows the lower frequency region the ε' decreased and at higher frequency remain constant. The similarly result observed in dielectric constant co related with frequency of nickel ferrite by Belavi et.al [44]. Fig.6(b) shows the distinction of dielectric loss tangent (tan™) with frequencies and showing the similar trend of ε'. It is seen that at a lower frequencies region the dielectric loss tangent is maximum and then decreases and remains constant at higher frequencies due to domain wall movement is upturned by the rotational movement of dipoles [45]. The electrical resistivity and dielectric dispersion in ferrite spinel are may be due to the interchange mechanism along with charge carriers at an A-site and B-site ions [46]. The dielectric constant of the prepared materials exhibits inversely proportional to square root of resistivity. The imaginary element of dielectric constant (ε") is estimated as the relation, $\varepsilon''=\varepsilon'\tan\delta$ whereas tan δ is be the tangent dielectric loss, these tangent dielectric loss shows that the function of energy loss between the applied electric field and prepared ferrite sample.

Fig.6(c) shows the different imaginary element of dielectric constant (ε") vs frequency of the Ni-Cd ferrite. The effect of annealing of temperature, addition of the impurities, and structural homogeneity of materials shows on the dielectric constant (ε") [47]. The dielectric losses are exhibits well supported to dominant of resonance at ferrite materials. The higher frequency range shows very less dielectric losses, it may be due to dominant motion and rotations of dipoles are changes due to the magnetic force [13]. The conduction mechanism of ferrite is studied by using complex impedance spectroscopy of the Ni-Cd ferrite system is shown in Fig.6(d). The electrochemical impedance spectroscopy (EIS) indicates that the real (Z') vs imaginary (Z") parts, EIS shows incomplete semicircles may due to the material possesses high resistance at lower frequencies. The diameter of the semicircle is varied with Cd^{2+} content in nickel ferrite due to the increase various resistance in the cadmium substituted nickel ferrite oxide materials.

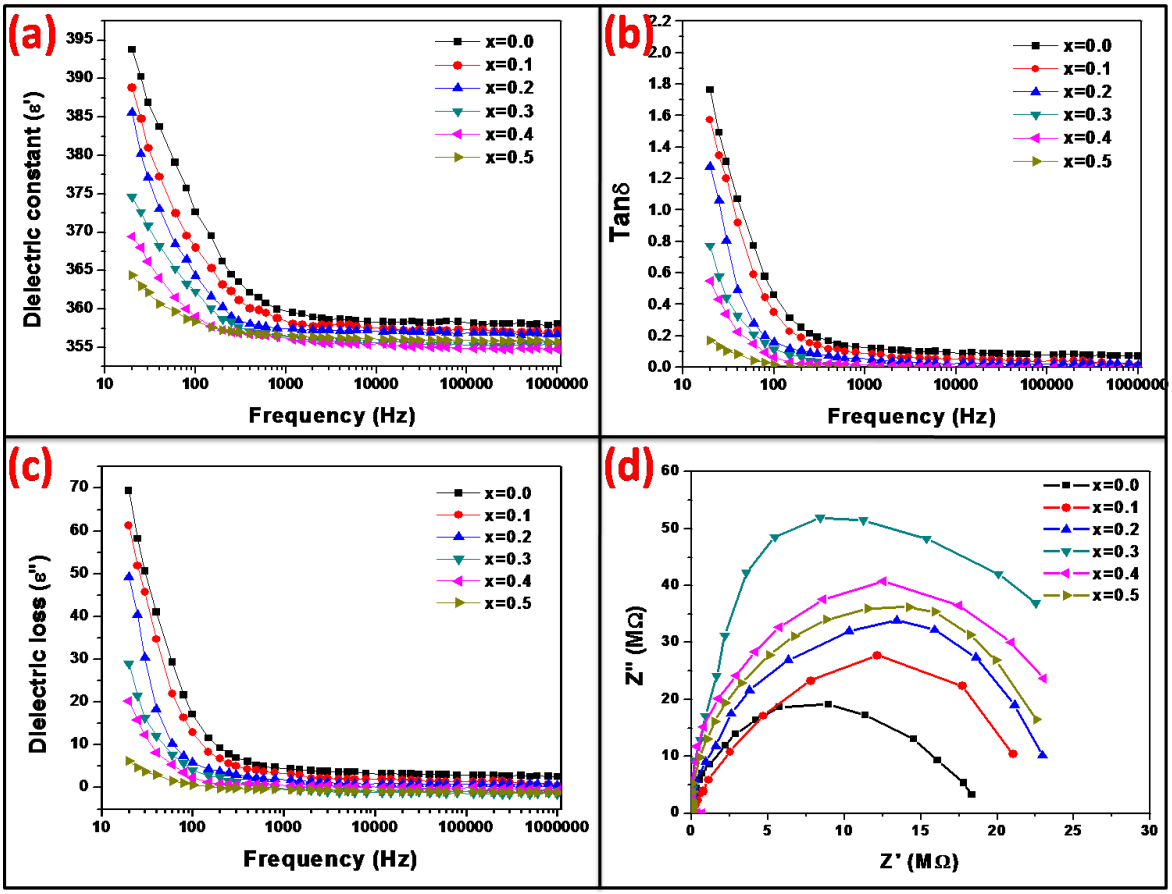

Figure 6. (a) Real part of dielectric constant with frequency, **(b)** Dielectric loss tangent (tan™) with frequency ,**(c)** Imaginary part of dielectric constant with frequency, **(d)** Nyquist plots of $Ni_{1-x}Cd_xFe_2O_4$ (x=0.0 to 0.5) ferrite system

4 Conclusions

Nanostructured $Ni_{1-x}Cd_xFe_2O_4$ (x=0.0 to 0.5) ferrite system was successfully synthesized by employing a solution combustion route. The XRD analysis revealed that all the prepared samples are single-phase cubic spinel crystal structure without any additional phase. The increases in lattice constant and an increase in crystallite size shows that the expansion of the unit cell may be due to different ionic radii. The SEM confirmations that all ferrite material samples exhibit an exaggerated continuous grain growth with grains containing some fine pores. The observed absorption bands of the FTIR spectra show the vibration of the tetrahedral and octahedral sites. The prepared cadmium substituted nickel ferrite oxide nano composite materials clearly indicate the semiconducting behaviours. The increasing constitutes of the cadmium in the nickel ferrite oxide composite to changes the activation energies of the paramagnetic region and it is shows they are higher than the paramagnetic region, the Curie temperature (*Tc*) decreases from 615 to 550°C temperature region with an increase in constitute of the Cd^{2+} in the nickel ferrite oxide. The magnetic behaviour of Cd^{2+} substituted nickel ferrite shows soft ferromagnetic nature. The saturation magnetization (Ms) and coercivity (Hc) were decreased with increase Cd^{2+} content be due to the increase of disordered spins which reduces the exchange interaction between tetrahedral and octahedral sites. The dielectric quantifications for all the ferrite material sample shows a conventional dielectric dispersion may be due to occurs space charge polarization. The impedance spectroscopy chemical analysis suggests a grain internal role in the conduction process.

Proceedings DOI: 10.21467/proceedings.118
ISBN: 978-81-947843-6-4

Series: AIJR Proceedings
ISSN: 2582-3922

Conflict of Interest: The authors declare that they have no conflict of interest.

References

[1] Teber A, Cil K, Yilmaz T, Manganese and zinc spinel ferrites blended with multi-walled carbon nanotubes as microwave absorbing materials, *Aerospace*, 4,2–18, (2017).

[2] J.M. Grenche, J. Teillet, H. Pascard, A mixed nickel-cadmium ferrite investigated by Mösbauer spectrometry ,*J. Magn. Magn. Mater*, 1402087-2088,(1995).https://doi.org/10.1016/0304-8853(94)01395-0.

[3] G. A. Sawatzky, F. Van Der Woude, A. H. Morrish, Mössbauer Study of Several, Ferrimagnetic Spinels, *Phys. Rev*, 187 , 747-757, (1969) .DOI:https://doi.org/10.1103/PhysRev.187.747.

[4] S. Singhal, S. Jauhar, N. Lakshmi, S. Bansal, Mn^{3+} substituted Co–Cd ferrites, $CoCd_{0.4}Mn_xFe_{1.6-x}O_4$ ($0.1 \leqslant x \leqslant 0.6$): Cation distribution, structural, magnetic and electrical properties, *J. Mol. Struct*, 1038 , 45–51, (2013). https://doi.org/10.1016/j.molstruc.2013.01.020

[5] C. Upadhjay, D. Mishra, H.C. Varma, S. Anaud, R.P. Das, Effect of Preparation Conditions on Formation of Nanophase Ni-Zn Ferrites Through Hydrothermal Technique, *J. Magn. Magn. Mater*,260,188-194, (2003). DOI: 10.1016/S0304-8853(02)01320-3

[6] S.E. Shirsath, B.G. Toksha, K.M. Jadhav, Structural and magnetic properties of In3+ substituted NiFe2O4, *Mater. Chem. Phys*. 117,163-168, (2009). https://doi.org/10.1016/j.matchemphys.2009.05.027

[7] S.M. Patange, S.E. Shirsath, S.S. Jadhav, K.M. Jadhav, Cation distribution study of nanocrystalline $NiFe_{2-x}Cr_xO_4$ ferrite by XRD, *magnetization and Mössbauer spectroscopy Phys. Status Solidi A*, 209,347-352, (2012). https://doi.org/10.1002/pssa.201127232.

[8] S.Hua, H. Zhang, X. Tang, X. Xiang, High-permeability and high-Curie temperature NiCuZn ferrite,*J. Magn. Magn. Mater*, 283,157-163, (2004) . DOI: 10.1016/j.jmmm.2004.05.017

[9] H. Zhong, H. Zhang, Effects of different sintering temperature and Mn content on magnetic properties of NiZn ferrites, *J. Magn. Magn. Mater*,283,247-250, (2004). https://doi.org/10.1016/j.jmmm.2004.05.029..

[10] S.E. Shirsath, S.S. Jadhav, B.G. Toksha, S.M. Patange, K.M. Jadhav, Influence of Ce^{4+} ions on the structural and magnetic properties of $NiFe_2O_4$, *J. Appl. Phys*. 110 (2011) 013914, https://doi.org/10.1063/1.3603004.

[11] S.M. Patange, S.E. Shirsath, B.G. Toksha, S.S. Jadhav, K.M. Jadhav, Electrical and magnetic properties of Cr3+ substituted nanocrystalline nickel ferrite, *J. Appl. Phys* ,106 ,023914, (2009). https://doi.org/10.1063/1.3176504

[12] Wang Z, Xie Y, Wang P, *et al*. Microwave anneal effect on magnetic properties of Ni0.6Zn0.4Fe2O4 nanoparticles,prepared by conventional hydrothermal method. *J Magn Magn Mater*,323,3121–3125, (2011).

[13] H.K.Dubey, P.Lahiri Synthesis, structural, dielectric and magnetic properties of Cd^{2+} based Mn nanosized ferrites, *Materials Technology*, (2020). DOI:10.1080/10667857.2020.1734728.

[14] T.T. Srinivassan, P. Ravindranathan, L.E. Cross, R. Ray, Studies on high-density nickel-zinc ferrite and its magnetic properties using novel hydrazine precursors, *J. Appl. Phys*, 63 ,3789, (1988). https://doi.org/10.1063/1.340615

[15] Y. Atassi, M. Tally, Low sintering temperature of Mg-Cu-Zn ferrite prepared by the citrate precursor method, *J. Iranian Chem. Soc*, 3,242-246, (2006).

[16] S.E. Shirsath, R.H. Kadam, A.S. Gaikwad, A. Ghasemi, A. Morisako, Effect of sintering temperature and the particle size on the structural and magnetic properties of nanocrystalline $Li_{0.5}Fe_{2.5}O_4$, *J. Magn. Magn. Mate*,323,3104-3108, (2011). https://doi.org/10.1016/j.jmmm.2011.06.065.

[17] K.S. Lohar, S.M. Patange, M.L. Mane, Sagar E. Shirsath, Cation distribution investigation and characterizations of $Ni_{1-x}Cd_xFe_2O_4$ nanoparticles synthesized by citrate gel process, *J. Mol. Struct*, 1032,105-110, (2013). https://doi.org/10.1016/j.molstruc.2012.07.055.

[18] Bhagwat S, Rao P. Study of dielectric properties of nano-crystalline Mn-Zn Ferrite. *J Appl Phys*,3, 01–06, (2013).

[19] A.Verma, T.C. Goel, R.G. Mendiratta, Dielectric properties of NiZn ferrites prepared by the citrate precursor method. *Mater Sci Eng B*, 60, 156–162, (1999).

[20] B.H. Devmunde, A.V. Raut, S.D. Birajdar, Structural, electrical, dielectric, and magnetic properties of Cd^{2+} substituted nickel ferrite nanoparticles, *J Nanoparticles* , 8, 1–8,(2016).

[21] [21] M. De, A. Mukherjee, H.S.Tewari, Characterization of cadmium substituted nickel ferrites prepared using auto-combustion technique, *Processing and Application of Ceramics*,9 ,193- 197, (2015). https://doi.org/10.2298/PAC1504193D.

[22] C.G. Winfrey, D.W. Eckart, A. Tauber, Preparation and X-ray diffraction data for some rare earth stannets, *J. Am. Chem. Soc*, 82, 2695–2697, (1960).

[23] A.L. Jadhav, S.V. Kambale, R.M. Kore, B.J. Lokhande, Capacitive Study of Nickel Oxide Thin Films Prepared by Spray Pyrolysis, *International Journal of Fracture and Damage Mechanic*, 5-2, 17-22,(2019).

[24] A.V.Raut, R.S.Barkule, D.R.Shengule, K.M. Jadhav, Synthesis, structural investigation and magnetic properties of Zn^{2+} substituted cobalt ferrite nanoparticles prepared by the sol–gel auto-combustion technique,J. Magn. Magn. Mater. 358-359 (2014) 87–92, https://doi.org/10.1016/j.jmmm.2014.01.039.

[25] Y.L. Huang, W.B. Fan, Y.H. Hou, K.X. Guo, Y.F. Ouyang, Z.W. Liu, Effects of intrinsic defects on the electronic structure and magnetic properties of $CoFe_2O_4$: A first-principles study, *J. Magn. Magn. Mater*, 429 , 263-269, (2017). https://doi.org/10.1016/j.jmmm.2017.01.043.

[26] V.S. Sawant, A.A. Bagade, S.V. Mohite, K.Y. Rajpure, Studies on structural and electrical properties of $Li_{0.5-0.5x}Co_xFe_{2.5-0.5x}O_4$ ($0 \leq x \leq 0.6$) spinel ferrite, *Physica B*, 474,47-52,(2015). https://doi.org/10.1016/j.physb.2015.06.005.

[27] A.M. Pachpinde, M.M. Langade, K.S. Lohar, S.M. Patange, S.E. Shirsath, Impact of larger rare earth Pr^{3+} ions on the physical properties of chemically derived $Pr_xCoFe_{2-x}O_4$ nanoparticles, *Chem. Phys*, 429, 20-26, (2014). https://doi.org/10.1016/j.chemphys.2013.11.018.

[28] R.Ahmad, I.H. Gul, M. Zarrar, H. Anwar, M.B.K. Niazi, A. Khan, Improved electrical properties of cadmium substituted cobalt ferrites nano-particles for microwave application,*J. Magn. Magn. Mater*, 405,28-35, (2016). https://doi.org/10.1016/j.jmmm.2015.12.019.

[29] A. Dais, R.L. Moreira, Conductivity behavior of *n*-type semiconducting ferrites from hydrothermal powders, *J. Mater. Res*, 12,2190, (1998). DOI: https://doi.org/10.1557/JMR.1998.0306.

[30] Y.P. Irkin, E.A. Turor, Sovt. Phys. JEPT. 33 (1957) 673.

[31] D. Ravinder, B. Ravi Kumar, Electrical conductivity of cerium substituted Mn–Zn ferrites, *Mater. Lett*, 57,1738-1742, (2003). DOI: 10.1016/S0167-577X(02)01060-1.

[32] G.R.Kumar, K.V.Kumar, Y.C.Venudhar, Synthesis, Structural and Magnetic Properties of Copper Substituted Nickel Ferrites by Sol-Gel Method. *Goldman, Modern Ferrite Technology, Van Nostrand Reinhold Company*, New York, NY, USA, 1990.

[33] R.N.Panda,J.C.Shih,T.S.Chin, Magnetic properties of nano-crystalline Gd- or Pr-substituted $CoFe_2O_4$ synthesized by the citrate precursor technique, *J. Magn. Magn. Mater*, 257, 79-86,(2003). https://doi.org/10.1016/S0304-8853(02)01036-3.

[34] L.Kumar,M.Kar, Effect of La^{3+} substitution on the structural and magnetocrystalline anisotropy of nanocrystalline cobalt ferrite ($CoFe_{2-x}La_xO_4$), *Ceram.Int*, 38,4771-4782, (2012). https://doi.org/10.1016/j.ceramint.2012.02.065.

[35]] V.R.K. Murthy, B. Viswanathan, Ferrite Materials, *Narosa Publishing House*, 1990.

[36] Y. Wang, F. Xu, L. Li, H. Liu, H. Qiu, Magnetic properties of La-substituted Ni–Zn–Cr ferrites via rheological phase synthesis, *J. Jiang, Mater. Chem. Phys*, 112,769-773, (2008). https://doi.org/10.1016/j.matchemphys.2008.06.032

[37] M.Ahmad, I.Ali, R. Grössinger, M. Kriegisch, F. Kubel, M.U. Rana, *J. Alloys Compnd*, 579, 57-64, (2013).

[38] S.S. Jadhav, S.E. Shirsath, S.M. Patange, K.M. Jadhav, Effect of Zn substitution on magnetic properties of nanocrystalline cobalt ferrite, *J. Appl. Phys*, 108,093920-093926,(2010). https://doi.org/10.1063/1.3499346

[39] S.R. Kulkarni, C.M. Kanamadi, B.K. Chougule, Dielectric and magnetoelectric properties of (x)Ni{sub 0.8}Co{sub 0.1}Cu{sub 0.1}FeâOâ/(1 - x)PbZr{sub 0.8}Ti{sub 0.2}Oâ composites, *Mater. Res. Bull*, 40 , 2064-2072, (2005). DOI: 10.1016/j.materresbull.2005.07.014

[40] J.C.Maxwell, Electricity and Magnetism, Vol. 1. *Oxford University Press, New York*, 88, (1973).

[41] K.W. Wagner, *Am. Phys*, 40, 817-819, (1973).

[42] C.G.Koops, On the Dispersion of Resistivity and Dielectric Constant of Some Semiconductors at Audiofrequencies, *Phys. Rev*, 83, 121-124, (1951). DOI:https://doi.org/10.1103/PhysRev.83.121.

[43] A.A.Bagade,K.Y.Rajpure,Studies on NO_2 gas sensing properties of sprayed $Co_{1-x}Mn_xFe_2O_4$ ($0 \leq x \leq 0.5$) spinel ferrite thin films, *Ceram. Int*. 41, 7394-7401, (2015). https://doi.org/10.1016/j.ceramint.2015.02.051.

[44] P.B.Belavi, G.N.Chavan, L.R.Naik, R. Somashekar, R.K. Kotnala, Structural, electrical and magnetic properties of cadmium substituted nickel–copper ferrites, *Materials Chemistry and Physics*, 132,138-144,(2012). https://doi.org/10.1016/j.matchemphys.2011.11.009.

[45] F. Muthafar, L. Sean, K.S. Kassim, Structural analysis, magnetic and electrical properties of samarium substituted lithium–nickel mixed ferrites, *J. Magn. Magn. Mater*, 324, 873-879, (2012). https://doi.org/10.1016/j.jmmm.2011.10.005.

[46] S.P. Yadav, S.S. Shinde, A.A. Kadam, K.Y. Rajpure, Structural, morphological, dielectrical and magnetic properties of Mn substituted cobalt ferrite, *J. Semicond*, 34, 093002, (2013).

[47] S.S. Bellad, B.K. Chougle, Composition and frequency dependent dielectric properties of Li–Mg–Ti ferrites, *Mater. Chem. Phys* , 66, 58-63,(2000). https://doi.org/10.1016/S0254-0584(00)00273-X.